Science of the Total Environment 684 (2019) 1–13

Contents lists available at ScienceDirect

Science of the Total Environment

journal homepage: www.elsevier.com/locate/scitotenv

A baseline of atmospheric greenhouse gases for prospective UK shale gas sites

Jacob T. Shaw [a,*], Grant Allen [a], Joseph Pitt [a], Mohammed I. Mead [a,1], Ruth M. Purvis [b], Rachel Dunmore [c], Shona Wilde [c], Adil Shah [a], Patrick Barker [a], Prudence Bateson [a], Asan Bacak [a], Alastair C. Lewis [b], David Lowry [d], Rebecca Fisher [d], Mathias Lanoisellé [d], Robert S. Ward [e]

[a] School of Earth and Environmental Science, University of Manchester, Manchester M13 9PL, UK
[b] National Centre for Atmospheric Science, University of York, Heslington, York YO10 5DD, UK
[c] Wolfson Atmospheric Chemistry Laboratories, Department of Chemistry, University of York, Heslington, York YO10 5DD, UK
[d] School of Earth Sciences, Royal Holloway University of London, UK
[e] British Geological Survey, Environmental Science Centre, Nicker Hill, Keyworth, Nottingham NG12 5GG, UK

HIGHLIGHTS

- 24-month statistical baseline for continuously-measured atmospheric CO_2 and CH_4
- Two UK sites being developed for shale gas exploration and hydraulic fracturing.
- Linked to prevailing local surface meteorology
- Diagnoses and interprets diurnal, day-of-week, and seasonal trends
- Guideline algorithm for identifying these statistically significant excursions

GRAPHICAL ABSTRACT

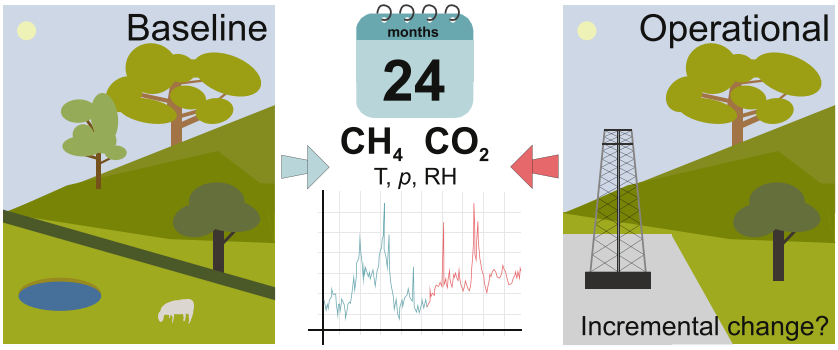

ARTICLE INFO

Article history:
Received 8 March 2019
Received in revised form 17 May 2019
Accepted 18 May 2019
Available online 21 May 2019

Keywords:
Hydraulic fracturing
Baseline
Methane
Carbon dioxide
Climatology
Shale gas
Greenhouse gases
Environmental baseline

ABSTRACT

We report a 24-month statistical baseline climatology for continuously-measured atmospheric carbon dioxide (CO_2) and methane (CH_4) mixing ratios linked to surface meteorology as part of a wider environmental baselining project tasked with understanding pre-existing local environmental conditions prior to shale gas exploration in the United Kingdom.

The baseline was designed to statistically characterise high-precision measurements of atmospheric composition gathered over two full years (between February 1st 2016 and January 31st 2018) at fixed ground-based measurement stations on, or near to, two UK sites being developed for shale gas exploration involving hydraulic fracturing. The sites, near Blackpool (Lancashire) and Kirby Misperton (North Yorkshire), were the first sites approved in the UK for shale gas exploration since a moratorium was lifted in England. The sites are operated by Cuadrilla Resources Ltd. and Third Energy Ltd., respectively.

A statistical climatology of greenhouse gas mixing ratios linked to prevailing local surface meteorology is presented. This study diagnoses and interprets diurnal, day-of-week, and seasonal trends in measured mixing ratios and the contributory role of local, regional and long-range emission sources.

* Corresponding author.
E-mail address: jacob.shaw@manchester.ac.uk (J.T. Shaw).
[1] Now at: Centre for Environmental and Agricultural Informatics, University of Cranfield, Cranfield, MK43 0AL, UK.

https://doi.org/10.1016/j.scitotenv.2019.05.266

The baseline provides a set of contextual statistical quantities against which the incremental impacts of new activities (in this case, future shale gas exploration) can be quantitatively assessed. The dataset may also serve to inform the design of future case studies, as well as direct baseline monitoring design at other potential shale gas and industrial sites. In addition, it provides a quantitative reference for future analyses of the impact, and efficacy, of specific policy interventions or mitigating practices. For example, statistically significant excursions in measured concentrations from this baseline (e.g. >99th percentile) observed during phases of operational extraction may be used to trigger further examination in order to diagnose the source(s) of emission and links to on-site activities at the time, which may be of importance to regulators, site operators and public health stakeholders. A guideline algorithm for identifying these statistically significant excursions, or "baseline deviation events", from the expected baseline conditions is presented and tested. Gaussian plume modelling is used to further these analyses, by simulating approximate upper-limits of CH_4 fluxes which could be expected to give observable enhancements at the monitoring stations under defined meteorological conditions.

1. Introduction

Greenhouse gas emissions associated with hydraulic fracturing of shale formations (commonly referred to as "fracking") for the commercial extraction of natural gas can occur via a variety of pathways. Over the full lifecycle of a typical well pad, emissions associated with on-site infrastructure such as flaring and generator use, transport, pipeline and gathering facility practices, and leakage (often referred to as fugitive emission) or venting, all contribute to the total carbon footprint of the activity (Burnham et al., 2012). Generating energy through the burning of natural gas, of which methane (CH_4) is typically the largest component, also directly produces carbon dioxide (CO_2). However, CO_2 is 28–34 times less potent as a greenhouse gas than CH_4 on a 100-year time scale (Myhre et al., 2013). Reductions in the global budget of both CO_2 and CH_4 emissions were shown by the International Panel on Climate Change (IPCC) to be fundamental in limiting global warming to below 1.5 °C from pre-industrial levels (Rogelj et al., 2018).

Natural gas extracted using hydraulic fracturing is often proposed as a less carbon-intensive alternative to coal in the UK energy sector and as a bridge to a lower carbon energy industry as renewable sources scale to meet a greater proportion of domestic demand. However, the relative climate impact of using gas instead of coal for energy generation depends on the proportion of CH_4 released to the atmosphere via leakage, intentional venting, or as a non-combusted component of flare and generator exhaust emissions. Total natural gas emissions to the atmosphere (irrespective of pathway) can be expressed as a percentage of total CH_4 produced over the lifecycle of a well or closed energy system. Beyond an estimated critical fugitive-emission threshold of 2–3% of total natural gas production (Jenner and Lamadrid, 2013), the significantly higher global warming potential of emitted CH_4 (versus CO_2) results in an equivalent net climate impact (per unit derived energy) as that of the coal industry (at least in the US context discussed by Jenner and Lamadrid, 2013). Current estimates of CH_4 emissions (whether by controlled venting, or as unwanted fugitive emission) from the now very large US shale industry range from ~1% to 12% of production with large variations attributed to individual sites and site practices (Howarth, 2015). A recent synthesis study by Littlefield et al. (2017) combined many separate measurement-led (top-down) studies across the full US natural gas supply chain to report a central estimate of fugitive emissions of 1.7% (with a 95% confidence level for the range 1.3% to 2.2%), compared with a US Environmental Protection Agency inventory (bottom up) estimate of ~1.4%. Another study estimated US supply chain CH_4 emissions equivalent to 2.3% of total production (Alvarez et al., 2018). These recent top-down estimates are close to the aforementioned critical threshold where shale gas would be considered to have a smaller impact on the climate than coal. The implications of such assessments are important factors in driving energy policy across all 2015 Paris Accord signatory nations considering exploiting (or continuing to exploit) their potential shale gas reserves.

Despite the convergence of many US fugitive emissions studies toward central estimates around 2%, there may yet be room for improvement in industrial practices to achieve lower rates of unwanted emission. A recent focus of US fugitive emission studies has been on the role of so-called "super-emitters" (e.g. Zavala-Araiza et al., 2015), which are classified as sites which have been observed to contribute significantly and disproportionately to total fugitive emission. A recent study by Zavala-Araiza et al. (2017) has linked super-emitting sites with abnormal upstream site practices and infrastructure malfunctions and proposes such sources as an explanation of an observed disagreement between component-based and site-based emission estimates. When informed by appropriate monitoring, improved site practices and regulations may aid in reducing CH_4 emissions by drawing together privately and publically funded measurement efforts and aligning them with successful mitigation policies (Konschnik and Jordaan, 2018).

The rapid development of the shale industry in the US since circa 2010 has also raised wider ranging environmental concerns beyond greenhouse gas emissions, including seismic geohazards (e.g. Frohlich, 2012; Kozłowska et al., 2018), impacts on local and regional air quality (Edwards et al., 2014; Field et al., 2014; Allen, 2016; Hildenbrand et al., 2016; Purvis et al., 2019) and groundwater pollution (e.g. Vidic et al., 2013; Darrah et al., 2014). This concern has attracted significant ongoing scientific attention and a great many measurement-led studies have now reported CH_4 emissions using a variety of methods, which include satellite remote sensing (e.g. Schneising et al., 2014), aircraft sampling (e.g. Peischl et al., 2018), mobile surveys (e.g. Lan et al., 2015), and long-term fenceline monitoring.

An atmospheric baseline aims to provide a set of measurements at a given location and over a period of time which are statistically representative of typical atmospheric conditions. These atmospheric conditions may be influenced by existing local, regional or global sources of chemical constituents. The baseline measurements presented here are intended to provide a set of conditions against which the impacts of operational shale gas extraction can be compared. To fully realise the potential this baseline offers, ongoing statistics must be established through long-term continuous observations, especially over the lifecycle of the activity of interest.

The authors aim to provide a framework upon which future greenhouse gas baseline monitoring sites can be established. We will outline a set of conclusions, drawn from our own experiences, which should assist in the installation of any long-term measurement facility prescribed for pre-existing greenhouse gas observations prior to the commencement of conventional or unconventional gas extraction. Further, we aim to provide a set of statistically-evidenced guidelines for the analysis of baseline data, to advise the detection of baseline deviation events.

2. Baseline site design

Cuadrilla Resources Ltd. and Third Energy Ltd. were granted Petroleum and Development Licenses by the UK government and given

permission for the construction of shale gas extraction facilities at sites on Preston New Road, near Little Plumpton, Lancashire and near Kirby Misperton, North Yorkshire respectively. For the remainder of this work these sites will be referred to as *PNR*, for the site in Lancashire, and *KM*, for the site in North Yorkshire. The KM greenhouse gas measurement facility was located on the Third Energy (KMA) site close to the Kirby Misperton village, whilst the PNR facility was located on a privately-owned dairy farm with approximately 250 cattle. Air quality and greenhouse gas measurement stations were positioned in the prevailing downwind direction from the infrastructure, as shown in Fig. 1, to optimise the monitoring of any potential operations in the future. Instrumentation was installed at both sites by January 2016 in mains-powered outdoor weatherproof enclosures. Greenhouse gases have been continuously monitored at both sites since installation. A two-year period (between 1st February 2016 and 31st January 2018) was analysed to determine the greenhouse gas baseline conditions. Two full years of data were chosen to allow for the assessment of inter-year variability and to yield robust statistical parameters on intra-yield variability.

Two different approaches to baseline site design were tested here. In the case of PNR, the monitoring site was located approximately 350 m to the east of the extraction infrastructure. In contrast, the KM facility was placed 50 m east of the unconventional shale gas exploration well. The proximity of the KM site to the well head likely provides a greater sensitivity to operational activity relative to that at PNR. CH_4 enhancements at PNR (due to operational activity) may prove harder to detect due to the greater distance between site and station. The larger distance may increase the dilution of emitted plumes prior to sampling. It should be noted, however, that the site at KM was also in close proximity to existing conventional gas extraction infrastructure which may complicate source identification in the future.

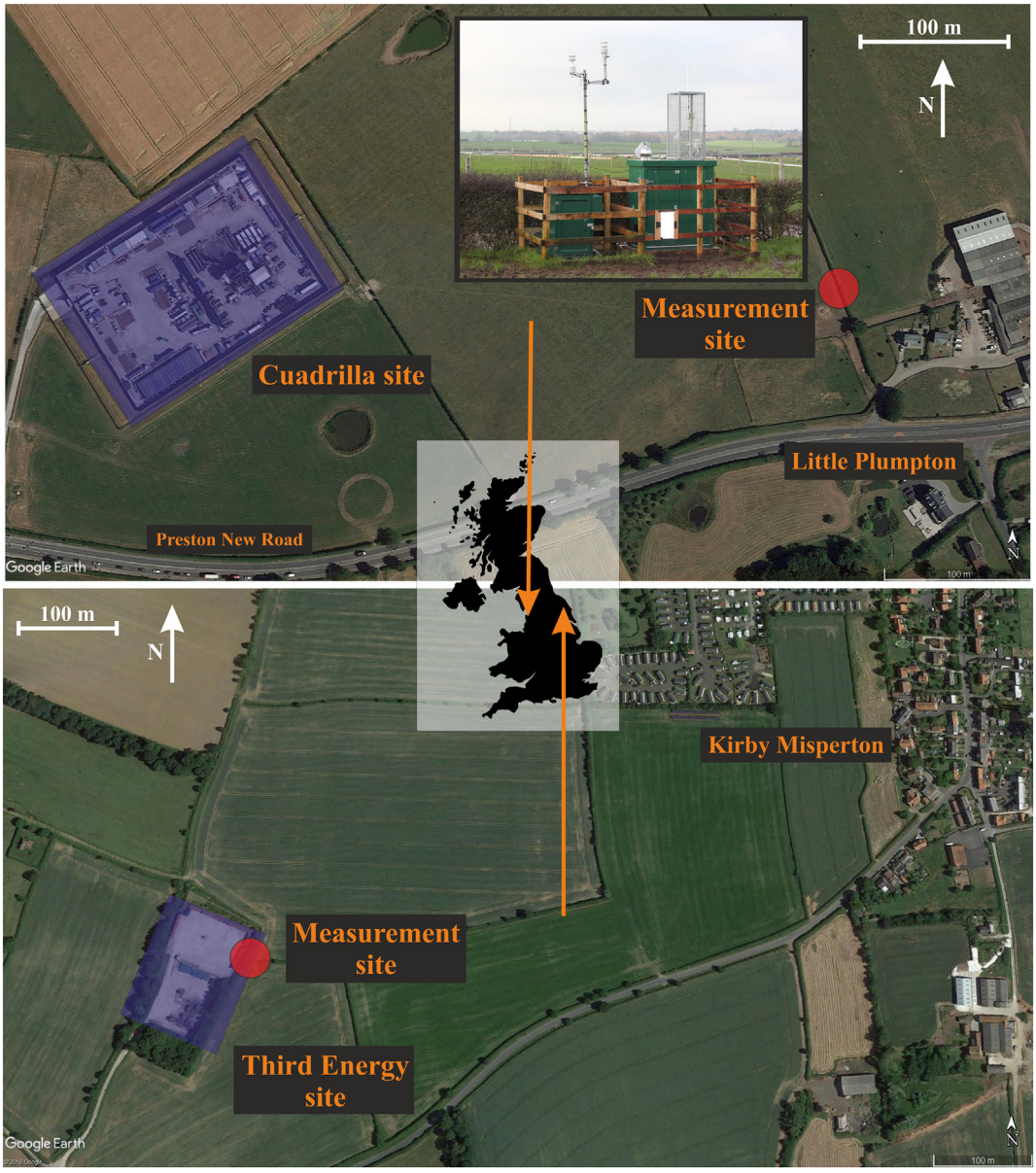

Fig. 1. Google Maps© images (images dated: top, 29/06/2018 and bottom, 01/07/2018) of the two measurement sites. North is at the top of both images. The site at PNR (top; red circle) is approximately 350 m east of the Cuadrilla site (top; blue square) and 100 m north of Preston New Road. The buildings to the east of the measurement site are part of a local dairy and cattle farming business and the M55 lies about 1.3 km to the north. The site at KM (bottom; red) is situated on the Third Energy site (bottom; blue square), 50 m east of the well head, and is approximately 600 m south west of Kirby Misperton village. A pre-existing conventional gas extraction facility is located approximately 80 m to the south east of the KM monitoring site. A second well site (not pictured) is also located approximately 800 m to the north-west of the monitoring station.

3. Instrumentation

Both fixed measurement sites contained identical high-precision in-situ CO_2 and CH_4 gas concentration analysers and thermodynamic (meteorological) stations, sampling continuously at 1 Hz, to provide consistent comparison and interpretation. Measurements of CO_2 and CH_4 were made using Ultra-portable Greenhouse Gas Analysers (UGGA; Los Gatos Research Inc., USA). Additional air quality parameters were measured simultaneously and will be reported in other work (Purvis et al., 2019). For a full list of on-site air quality instrumentation, please refer to the Supplementary Information, or to Purvis et al. (2019). Additional greenhouse gas measurements, made as part of multiple mobile monitoring surveys throughout the baseline period, will also be reported in future work. This work is all part of a wider environmental monitoring programme that also included ground/surface water and seismicity monitoring (Ward et al., 2017; Ward et al., 2018).

Three UGGA instruments were deployed throughout the baseline period; they are nominally referred to as α, β, and γ for the purposes of this work. UGGA-β was installed at KM for the entire duration of the baseline measurements. UGGA-γ was deployed at PNR from 1st February 2016 until 9th January 2018 when it was removed and replaced by UGGA-α due to cell contamination. UGGA-α remained in place at PNR until the end of the baseline period. Data from all three instruments were individually corrected for the influence of water vapour based on laboratory testing of each unit, following the procedure described by O'Shea et al. (2013).

Quality assurance (QA) and quality control (QC) procedures were routinely performed for all aspects of data measurement, including; equipment evaluation, site operation and maintenance, and data review and ratification. All instrument calibrations were traceable through an unbroken chain to international standards to maintain a high accuracy and provide known uncertainties in the recorded data. The UGGA instruments were calibrated in the field using gas standards containing known mixing ratios traceable to the World Meteorological Organisation (WMO) scales for CO_2 (X2007) and CH_4 (X2004A). These calibrations involved sequentially sampling a low concentration standard (~400 ppm CO_2, ~2 ppm CH_4) followed by a high concentration standard (~600 ppm CO_2, ~5 ppm CH_4), enabling for the determination of both the offset and slope (gain factor) of the instrument response. Calibrations were performed during regular site maintenance visits using either calibration gas from 40 L lab standards (filled by Deuste, Steininger GmbH, Germany, and certified on the WMO scale by EMPA, Switzerland) decanted into 6 L SilcoCan canisters (Thames Restek, UK) for transport, or from 5 L cylinders that could be transported to site (filled at the University of York, UK and certified on the WMO scale by EMPA, Switzerland). Both the 40 L and 5 L cylinders were made from 6061 aluminium alloy (Luxfer, UK) and fitted with brass D200 valves (Rotarex, Luxembourg) containing a PCTFE seat. Single-stage diaphragm brass regulators (TESCOM, UK) were used to deliver gas from the 40 L lab cylinders, and two-stage diaphragm 1000-series regulators (Calgaz, UK) were used in conjunction with the 5 L cylinders.

Significant drifts of over 0.5 ppm for CO_2 and 10 ppb for CH_4 were observed in the 5 L cylinders with respect to the 40 L lab standards over a period of 11 months. These drifts were thought to be associated with the presence of a small quantity of water vapour (~200–300 ppm) in the cylinders. Repeat measurements of the 5 L cylinder concentrations, with respect to the stable 40 L cylinder concentrations, were used to derive WMO-traceable mixing ratios as a function of time to capture the drift in these cylinders. The 40 L lab standards were certified by EMPA in both June 2016 and July 2018 and showed negligible drift during this period.

The calibrations for two of the UGGA instruments (UGGA-α and UGGA-β) were highly correlated with cell temperature. The calibration data for UGGA-γ was less obviously correlated to cell temperature but drifted linearly over time. Calibration corrections were therefore applied to the three UGGAs separately according to their individual characteristics. This clearly highlights the necessity of routine and regular calibrations for all long-term field-deployed instrumentation, where high accuracy is required, even for those that are manufactured to the same standards.

Atmospheric composition data used in this work, alongside meteorological variables, are publicly available on the Centre for Environmental Data Analysis Archive (CEDA Archive; http://www.ceda.ac.uk/); metadata concerning data precision and usage guidance are also provided. Over time the baseline dataset may be expected to display internally consistent or contrasting behaviour in the context of both natural background (meteorological and seasonal), local (nearby), and regional (cumulative national) source profiles. Such analysis yields receptor relationships with respect to time of day, day of week, month of year, and how these relate to wind direction and wind speed (and therefore upwind emission sources). By comparing these statistical regimes, the nature of any observed systematic differences or variability was qualitatively deconvolved.

4. Results and discussion

A summary of the statistical analysis of the greenhouse gas observational data obtained at the two baseline monitoring stations is discussed in this section. Firstly, the climatology is examined to account for the placement of the monitoring site, and to provide an understanding of the climatological conditions likely to occur once operational activities commence. By understanding the statistical range of the pre-existing climatology, a set of threshold criteria that enables for the identification of baseline deviation events, such as emissions of CH_4, tailored to each site, is then defined and tested.

The authors would like to stress that any guidelines presented as part of this work may not be directly applicable to all shale gas extraction monitoring facilities, as site-by-site consideration is required for aspects such as site positioning and site-specific sources of extraneous emissions. However, the statistical and analytical method described here could be used to derive a meaningful climatology for any baseline station.

4.1. Wind climatology

Local surface wind direction and wind speed help to inform local and regional air mass history, providing an indication of potential emissions that influence the sampled air upwind. Wind rose plots allow for a direct evaluation of wind direction and wind speed at a stationary receptor site. The frequency of wind speeds occurring in defined ranges and in defined directions are plotted, illustrating the prevalent wind directions and wind speeds.

Fig. 2 shows wind roses for the PNR (left panel) and KM (right panel) sites from 1st February 2016 to 31st January 2018. As expected, the dominant wind direction at the PNR site was from the west; consistent with the location of this site on the west coast of the UK mainland, which is typically exposed to flow associated with the Atlantic mid-latitude storm track. The strongest winds were also typically observed from a westerly direction. Westerly winds, bringing air masses from the Atlantic, would be expected to be relatively well-mixed and broadly characteristic of the average Northern Hemisphere background greenhouse gas composition at the time.

The principal wind direction for the site at KM was from the south-west. Whilst the greater proportion of strong winds were observed from this direction at KM, the relative frequency of such winds was far lower than those for the PNR site. This is consistent with the position of KM near to the eastern coast of the UK. Sampling of air masses at the KM site may therefore be expected to contain enhanced concentrations of CH_4 representative of the range of UK land-based natural and anthropogenic sources over which the air has passed.

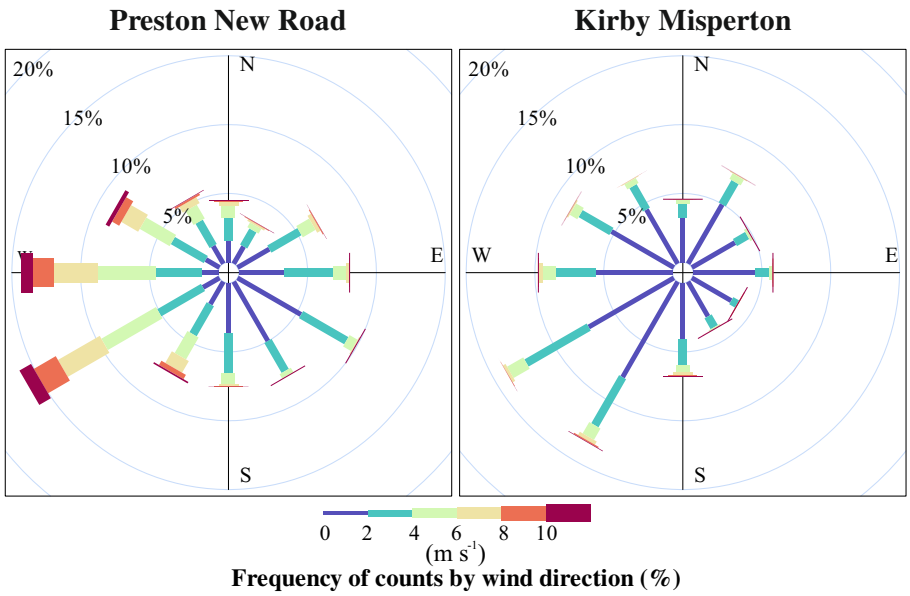

Fig. 2. Wind rose plots for the sites at Preston New Road (left) and Kirby Misperton (right). The frequency of counts of wind speeds (m s^{-1}) are shown as a function of direction for the measurement period 01/02/2016 to 31/01/2018. The maximum wind speed recorded at PNR was 21.7 m s^{-1} and at KM was 18.3 m s^{-1}. The mean wind speed at PNR was 3.7 m s^{-1} and at KM was 1.8 m s^{-1}. Year-to-year variations in wind direction and wind speed statistics are not illustrated here but were low.

4.2. Greenhouse gas baseline measurements

Fig. 3 shows time series of measured six hour-average ambient CO_2 and CH_4 mixing ratios (defined as the ratio of the number of moles of CO_2, or CH_4, to the number of moles of air) at the PNR and KM sites. These time series are useful to gain a broad overview of both CO_2 and CH_4 baseline mixing ratios and provide a quick-look assessment of the variability as a function of time. Average baseline mixing ratios of roughly 400 ppm CO_2 and 2 ppm CH_4, consistent with other sites in the Northern Hemisphere (Dlugokencky, 2019), were observed throughout the time period.

Similar trends in CH_4 and CO_2 mixing ratios were observed at both PNR and KM. Seasonal variations in CO_2 mixing ratios were clearly visible at both sites with higher average values in winter and lower values observed in summer due to the seasonal fluctuation in biosphere uptake. The seasonal variation in CH_4 mixing ratios (largely driven by changes in oxidative sink), whilst present, was less obvious; the influence of local sources, apparent from the large day-to-day variability, was far more dominant. There were periods where short-term enhancements were observed to co-occur at both sites (e.g. 8th and 9th April 2017). Trajectory analysis confirmed that such periods were consistent with regionally consistent meteorological flow conditions in which the measurements were influenced by air masses sourced from continental Europe to the east and south-east (usually during high pressure blocking events when pressure centres existed to the south and east of the UK).

The variability in CH_4 mixing ratio was greater at PNR than at KM. This was likely due to the location of the PNR measurement site on a dairy farm, which represented a significant continuous source of CH_4 emissions. The opposite was true for CO_2, with greater variations in CO_2 mixing ratios observed at KM. This was attributed to the more frequent sampling of air masses sourced from over the land at KM (due to the prevailing south-westerly wind direction), relative to PNR. Both CO_2 emission sources, and sinks related to biospheric uptake, are largely land-based, especially during the spring and summer.

These time series could be used as a crude baseline tool by allowing for comparisons of any future measurements against those observed here for the baseline period. However, this type of data provides only a cursory evaluation of the measurements and does not account for any localised influences on the observations. Interferences from farming activities for example, could bias the conclusions drawn from a simple comparison of concentration time series, particularly for CH_4.

The influence of localised sources of pollution on the observed data was examined by separating the measurements according to the wind direction. This provides further insight with respect to procuring a wind-dependent baseline concentration for both CO_2 and CH_4. Concentration-wind rose plots for CH_4 at both PNR and KM are shown in Fig. 4. Concentration-wind rose plots are similar to the wind rose plots presented in Fig. 2. However, rather than plotting the frequency of wind speeds occurring in different categories, the frequency of mixing ratio measurements in different ranges are plotted. This allows for an assessment of the influence that wind direction has on the observed mixing ratios at the baseline sites. As for the wind-rose plots (Fig. 2), the radii of the wedges represent the frequency of measurements in that wind direction. Mixing ratios are illustrated by the coloured scale. Fig. 4 clearly illustrates that higher mixing ratios of CH_4 ($CH_4 > 2200$ ppb) were associated with easterly winds at PNR and were likely as a result of the nearby dairy farm. Air masses with the lowest CH_4 mixing ratios at PNR ($CH_4 < 2000$ ppb) were observed from the west, consistent with background air sourced from the mid-Atlantic. The same was not true for the site at KM where the observations of CH_4 mixing ratios exhibited a smaller dependence on wind direction.

Concentration-wind rose plots for CO_2 are provided in Fig. 5. Higher CO_2 mixing ratios ($CO_2 > 420$ ppm) were consistently associated with easterly winds at PNR. The independence of CO_2 mixing ratios with season suggests that these emissions were locally sourced and associated with the nearby dairy farm upwind for this wind direction. The lowest CO_2 mixing ratios at PNR ($CO_2 < 410$ ppm) were again associated with westerly winds from over the mid-Atlantic. Mixing ratios of CO_2 at KM were marginally greater from the north-east but were less clearly dependent on wind direction compared with the observations at PNR. This is consistent with the large number of nearby potential sources of CO_2 at the KM site, including a static caravan park to the north, Kirby Misperton Village to the north east and a pig farm around 400 m to the north-west (also a potential source of CH_4).

Considering the high variability in observed background greenhouse gas concentrations corresponding to different wind directions (particularly at PNR) an overall baseline for CH_4 and CO_2 mixing ratios was

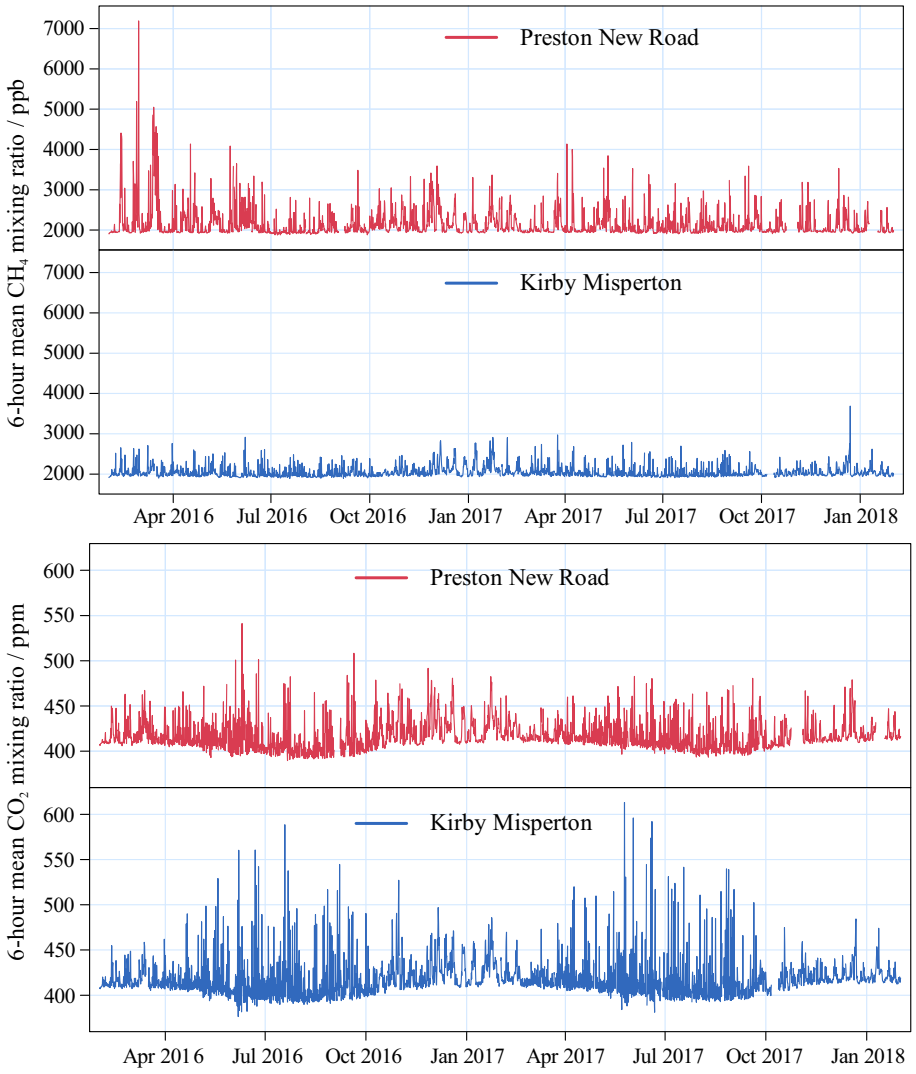

Fig. 3. Time series plots of 6-hour mean CH_4 and CO_2 mixing ratios for the sites at Preston New Road and Kirby Misperton for the measurement period 01/02/2016 to 31/01/2018.

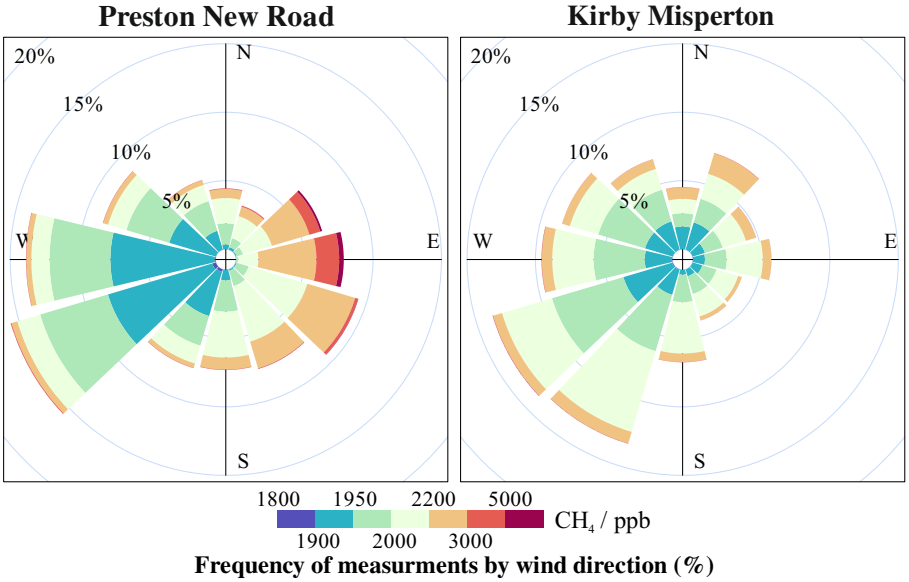

Fig. 4. Concentration-wind rose plots for one-minute averaged CH_4 mixing ratios as a function of wind direction at Preston New Road and Kirby Misperton for the measurement period 01/02/2016 to 31/01/2018.

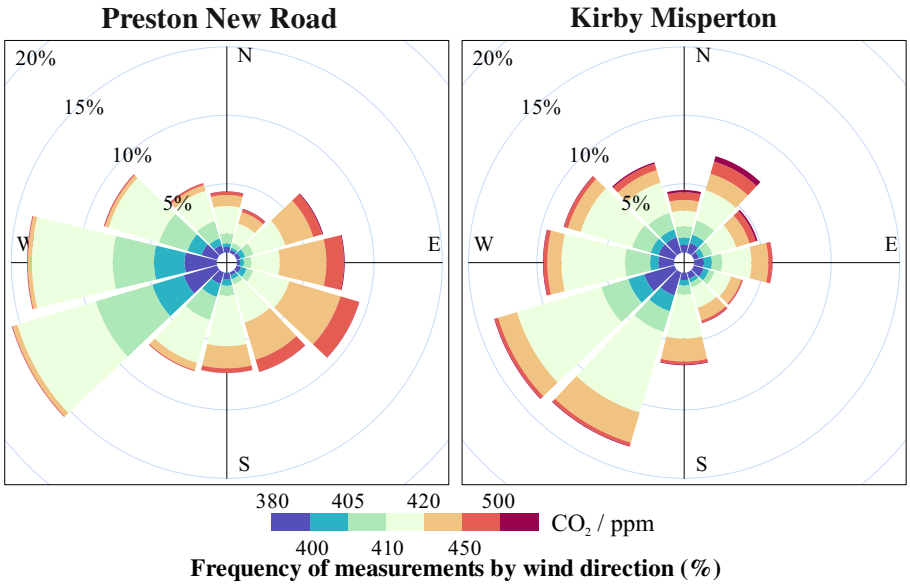

Fig. 5. Concentration-wind rose plots for one-minute averaged CO_2 mixing ratios as a function of wind direction at Preston New Road and Kirby Misperton for the measurement period 01/02/2016 to 31/01/2018.

deemed inappropriate. Rather, different baselines for different meteorological conditions were judged to be more applicable for identifying future baseline deviation events. Tables 1 and 2 provide values of statistical parameters for baseline one-minute averaged CH_4 and CO_2 mixing ratios, separated by wind direction. These tables reflect the data presented in Figs. 4 and 5 but are categorised into the four cardinal directions (±45°) for ease of interpretation.

Accounting for the influence of wind direction and local and regional sources of CH_4 and CO_2 allows for a much more in-depth baseline interpretation. Measured CH_4 mixing ratios, at PNR in particular, were greatly impacted by wind direction; much larger mixing ratios were observed for winds from the north and east compared to those from the south and west.

Clearly, in the context of diagnosing future emission events, wind direction must be considered. For a simple example, a measured CH_4 mixing ratio of 2700 ppb at PNR would be just above the 75th percentile if the wind were from the east, and would be highly unlikely to be associated with shale gas operations as air would not have passed over the site prior to measurement. However, the same measurement under westerly winds would exceed the 99th percentile and would therefore have a significant possibility of being associated with emissions from the site upwind.

The maximum CH_4 and CO_2 mixing ratios reported in Tables 1 and 2 were due to extremely short time periods likely associated with transitory events (e.g. a cow passing within meters of the instrument inlet). Such events are not meaningful in the context of a local area baseline. These singular data-point maxima were therefore not representative of the typical climatological statistical limit of greenhouse gas mixing ratios during the baseline period. The 99th percentile mixing ratios should be used as a more instructive substitute for an upper limit of measurements at the monitoring stations.

The minimum CH_4 and CO_2 mixing ratios recorded during the baseline period were extremely low; CH_4 mixing ratios below 1870 ppb were measured multiple times during July 2016 at PNR. 10-day back trajectory analyses for these periods suggest that these were associated with large scale subsidence of remote Arctic upper tropospheric air prior to sampling. The low CH_4 mixing ratios (CH_4 = 1857 ppb) recorded at PNR were also consistent with similarly low mixing ratios recorded at the Mace Head Atmospheric Research Station, Republic of Ireland (CH_4 = 1850 ppb; Prinn et al., 2018) during the same periods

Table 1
One-minute averaged CH_4 mixing ratios under different wind conditions at Preston New Road and Kirby Misperton during the measurement period 01/02/2016 to 31/01/2018. The wind directions are divided evenly into the four cardinal directions i.e. south refers to wind directions of 180° ± 45°.

Statistic	Baseline CH_4 mixing ratio/ppb							
	Preston new road (PNR)				Kirby Misperton (KM)			
	North	East	South	West	North	East	South	West
Maximum	30,180	70,690	16,170	10,480	6895	5145	34,180	41,420
P_{99}[a]	3079	6156	2779	2544	2767	2665	2632	2627
P_{95}	2458	3998	2424	2128	2473	2360	2269	2256
P_{90}	2274	3252	2290	2034	2336	2231	2170	2136
P_{75}	2098	2617	2116	1973	2093	2092	2076	2029
Mean ± 1σ	2081 ± 324	2538 ± 929	2076 ± 218	1979 ± 139	2061 ± 197	2057 ± 154	2049 ± 177	2021 ± 222
Median (P_{50})	2000	2273	2014	1949	1977	2009	2012	1977
P_{25}	1962	2095	1961	1935	1943	1961	1971	1950
$P_{0.1}$	1906	1934	1870	1871	1897	1894	1894	1891
Minimum	1873	1871	1857	1857	1866	1879	1870	1863

[a] P_i refers to the i^{th} percentile e.g. P_{90} refers to the 90th percentile.

Table 2
One-minute averaged CO_2 mixing ratios under different wind conditions at Preston New Road and Kirby Misperton during the measurement period 01/02/2016 to 31/01/2018. The wind directions are divided evenly into the four cardinal directions i.e. south refers to wind directions of 180° ± 45°.

Statistic	Baseline CO_2 mixing ratio/ppm							
	Preston new road (PNR)				Kirby Misperton (KM)			
	North	East	South	West	North	East	South	West
Maximum	709	719	586	886	724	661	761	738
P_{99}[a]	489	493	477	442	549	508	485	478
P_{95}	450	469	454	421	488	460	443	442
P_{90}	436	457	443	417	462	445	434	430
P_{75}	423	441	428	413	431	427	425	419
Mean ± 1σ	418 ± 18	430 ± 21	420 ± 17	409 ± 10	424 ± 31	420 ± 23	418 ± 18	414 ± 16
Median (P_{50})	413	427	416	409	413	416	416	414
P_{25}	408	416	409	403	406	406	408	406
$P_{0.1}$	388	390	391	388	389	376	378	389
Minimum	380	379	384	382	373	366	364	373

[a] P_i refers to the i^{th} percentile e.g. P_{90} refers to the 90th percentile.

(see Supplementary Information). The 0.1th percentile is therefore a better representation of the tropospheric minimum CH_4 and CO_2 mixing ratios observed at the monitoring stations as it avoids these exceptional circumstances.

Whilst wind direction was one dominant factor in the statistical assessment of measured CH_4 and CO_2 mixing ratios, other factors related to upwind variability in existing emissions must be considered. The values provided in Tables 1 and 2 are representative of the full two-year measurement period. However, scrutiny of Fig. 3 shows that there were temporal variations in the data as well, with potentially significant variability in measured CO_2 mixing ratios throughout the year.

Fig. 6 shows a series of dynamic baselines at PNR and KM under westerly wind conditions – the primary wind direction of interest for examining emissions from the shale gas sites. A dynamic baseline takes into account the temporal variations on different time scales; month-to-month, day-to-day and hour-to-hour. This facilitates a more resolved use of the baseline specific to the nature of prevailing conditions at the time of measurement when assessing the potential explanation for signals observed during any operational phase (i.e. during drilling, hydraulic fracturing and gas extraction). Dynamic baseline plots for other wind directions for each site are provided in the Supplementary Information. In these plots, the median mixing ratios of CH_4 and CO_2 are illustrated as a function of time. Parameters, including the 25th, 75th, 10th and 90th percentiles, may allow for future identification of baseline deviations at different points in time. These plots provide extra temporal detail which is highly advantageous for those chemicals which vary considerably in concentration diurnally, daily or seasonally.

For example, there were clear diurnal changes in both CH_4 and CO_2 at KM, with greater variability observed at night than during the day. This was likely due to changes in the boundary layer conditions with night-time pooling of local emissions in shallow boundary layers. Distinct diurnal changes in variability were not present at PNR due to it being more consistently exposed to marine air. A spike in CH_4 was observed at PNR at approximately 5 pm local time, which may be consistent with an unconfirmed daily procedure at the nearby dairy farm (e.g. collection of cattle for milking, which is known to happen daily at around this time).

Comparisons of westerly dynamic baseline plots with those for other wind directions (see Supplementary Information) definitively illustrates the lower temporal variability in measurements associated with westerly winds. Measured mixing ratios for northerly and easterly winds were subject to much larger variability. This provides further evidence for the need for careful positioning of monitoring stations to

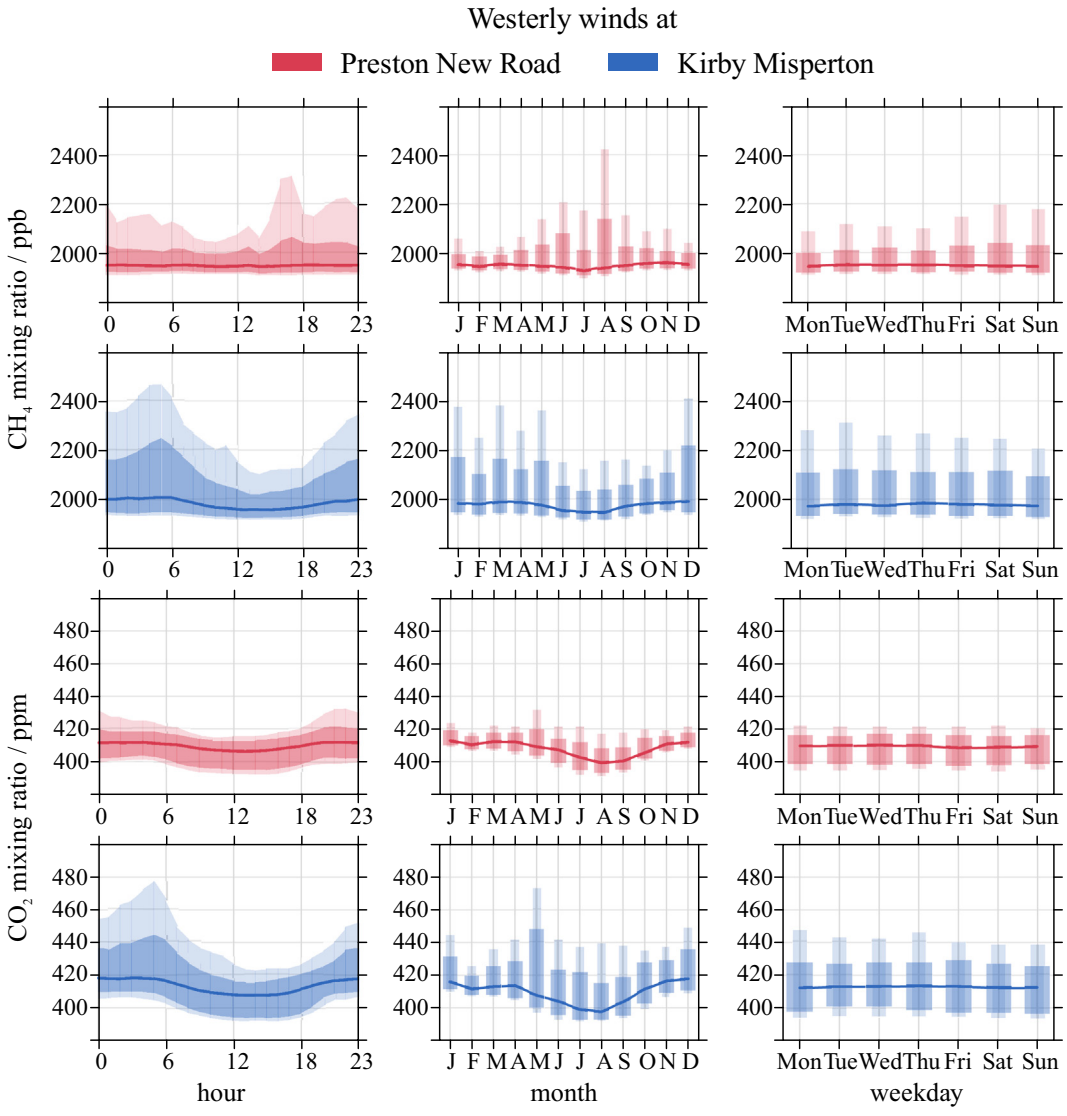

Fig. 6. Dynamic baseline plots for one-minute average CH_4 and CO_2 at PNR and KM under westerly wind conditions for the measurement period 01/02/2016 to 31/01/2018. The darker shaded areas represent the interquartile range (from the 25th to the 75th percentiles). The lighter shaded regions represent the range from the 10th to the 90th percentiles.

ensure that sampling is carried out at a position downwind of the facility of interest in a prevailing wind direction. Where possible it would be preferential to locate the monitoring station away from the compounding contributory effects of strong local and regional sources of pollution that would otherwise confound the detection of emission events. For example, whilst it was not possible to completely eliminate the influence of all local sources, situating the PNR measurement station between the shale gas facility and the dairy farm allowed for distinctions between the two potentially major CH_4 sources to be made through observations of wind direction. Positioning the monitoring station to the east of the shale gas site at PNR allowed for the sampling of a more stable and unpolluted background of air masses arriving on westerly winds.

Associations between baseline deviation events and emissions due to shale gas extraction may not always be possible using the above reference plots alone, even when considering statistical variations due to both wind direction and time-of-day, -week, or -year. Well-mixed and polluted air masses, with high concentrations of both CH_4 and CO_2, may well result in the identification of false positives when testing for emissions. Similarly, certain meteorological conditions may lead to the build-up of CH_4 and CO_2 concentrations until they exceed any threshold values. Tracer-tracer analyses can provide an additional diagnostic evaluation of emissions events and allow for distinguishing locally emitted CH_4 from well-mixed, or stationary, air masses high in both CH_4 and CO_2.

Fig. 7 shows the observed correlation between CO_2 and CH_4 mixing ratios at PNR and KM for the baseline period under all wind conditions (top row) and under westerly wind conditions (bottom row). These plots are useful for visualising the scatter of the data. Warmer coloured (red) data points show a higher frequency of one-minute averaged measurements whilst cooler coloured (blue) data points show that very few observations were made within those values.

Fig. 7 shows that there were similarities between the two sites. The most frequent measurements occurred at low CO_2 (approximately 400–450 ppm) and low CH_4 (approximately 2000 ppb) mixing ratios. A dominant mixing line (approximately indicated by the purple lines) was observed at each site, illustrating a typical trend in simultaneously measured values. However, there were also contrasts in the observations at the two sites. As discussed previously, the variation of CH_4 at PNR was much greater than that at KM. The blurring of the prominent mixing line along the x-axis at PNR was likely due to the influence of locally emitted CH_4, or from polluted air masses from more distant regional sources. On the other hand, the variability in CO_2 at KM was greater than that observed for PNR, consistent with Fig. 3.

In practice, these plots allow for the expected CO_2 vs CH_4 values to be evaluated. A prominent feature of the plot for KM is the data at approximately 420 ppm CO_2, and between 5000 and 50,000 ppb CH_4. This mixing line clearly highlights an excursion in the mixing ratios of CH_4 relative to CO_2 that were outside of the general trend. Events such as these likely indicate examples of cold venting of CH_4 from the pre-existing conventional gas well-head to the south west of the monitoring station. Excursions from the general trend such as these could also be indicative of future emissions at either site.

4.3. Identifying baseline deviations

The analyses performed above provide a set of statistical quantities for the pre-existing local greenhouse gas environmental conditions

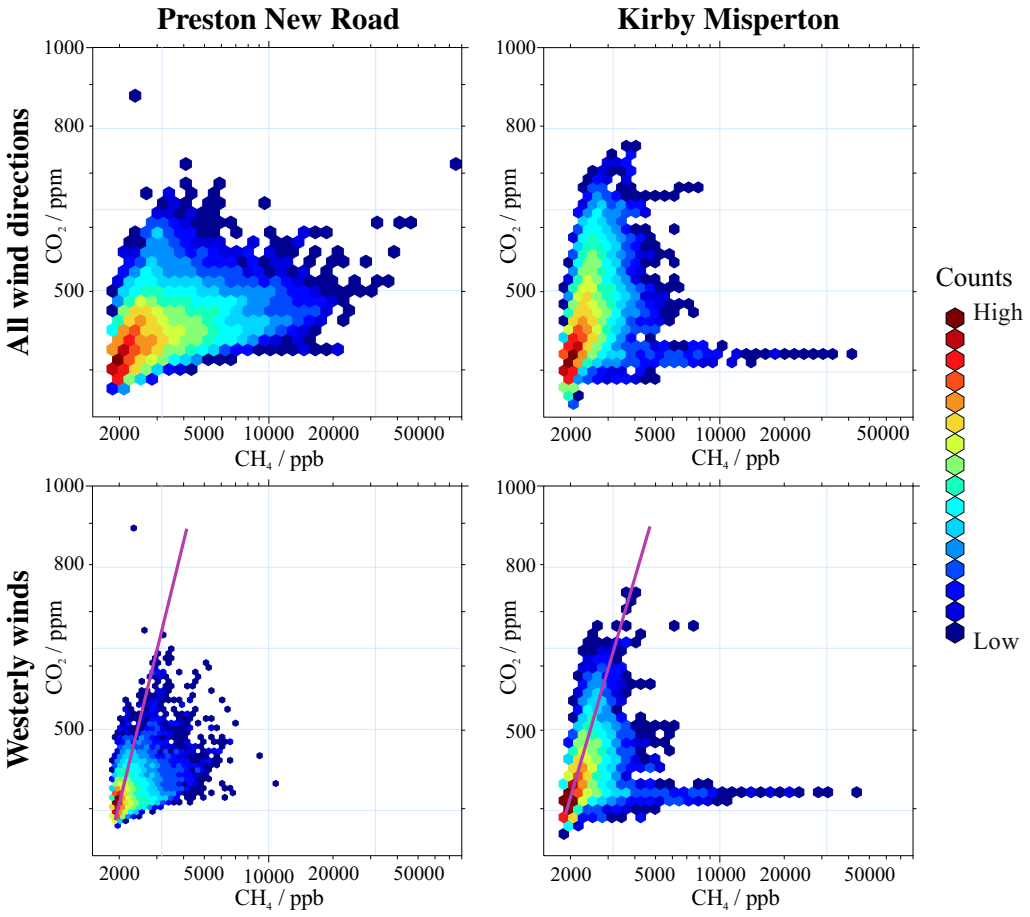

Fig. 7. Top row: minute average CO_2 vs CH_4 mixing ratios at PNR and KM under all wind directions for the measurement period 01/02/2016 to 31/01/2018. Bottom row: minute average CO_2 vs CH_4 mixing ratios at PNR and KM under westerly wind conditions only for the measurement period 01/02/2016 to 31/01/2018. The colour of the hexagonal data points indicates the frequency of measurements; dark red indicates a large number of one-minute data points, dark blue indicates only a single one-minute data point. Approximate dominant mixing lines are indicated by the purple lines on the bottom panels.

prior to hydraulic fracturing and shale gas extraction for each site. These climatologies can be used to derive a framework against which incremental impacts of new activities at the sites could be assessed. More importantly, the data could be used to outline guidelines for the potential investigation of CH_4 emissions, intentional or otherwise, which could be associated with identified baseline deviation events. In order for such guidelines to be routinely applicable they need to be capable of distinguishing cold venting activities from other potential CH_4 sources. However, the criteria must also be lenient enough to correctly identify all venting pathways, including those associated with flaring.

Fig. 8 depicts a recommended process chart for the identification of extreme or significant baseline excursions which could be associated with operational activity for a specific site. A combination of meteorological and chemical parameters was used to reduce the possibility of influences from other sources. The ratio of $[CH_4]$:$[CO_2]$ at each time was calculated for each site to provide some indication of the influence of regional pollution. A new variable, the product of wind speed and CH_4 enhancement, was also calculated to allow for the elimination of meteorologically stagnant periods with extensive CH_4 pooling. The dynamic baseline dataset was processed to yield a set of threshold criteria based on the 99th percentile of these, and other variables, with the aim that these threshold criteria could be applied to future measurements at each site.

These criteria were applied to the baseline dataset to determine their utility in attributing emission events. As the baseline data represents data recorded prior to operational activity at the sites, the criteria would be expected to return minimal exceedances. Firstly, hourly averages of each variable were calculated for the target dataset. The wind direction was then limited to those winds passing directly from the west, over the shale gas sites; i.e. those with a direction >225° and <315°. The 99th percentile threshold criteria were then applied to $[CH_4]$, ws × $[CH_4]_e$ and the ratio $[CH_4]$:$[CO_2]$.

Nine one-hour periods at PNR and seven one-hour periods at KM exceeded the criteria during the two-year period, corresponding to approximately 0.05% of the data from each site. The exceedance of several one-hour periods at PNR indicate that the threshold criteria are not

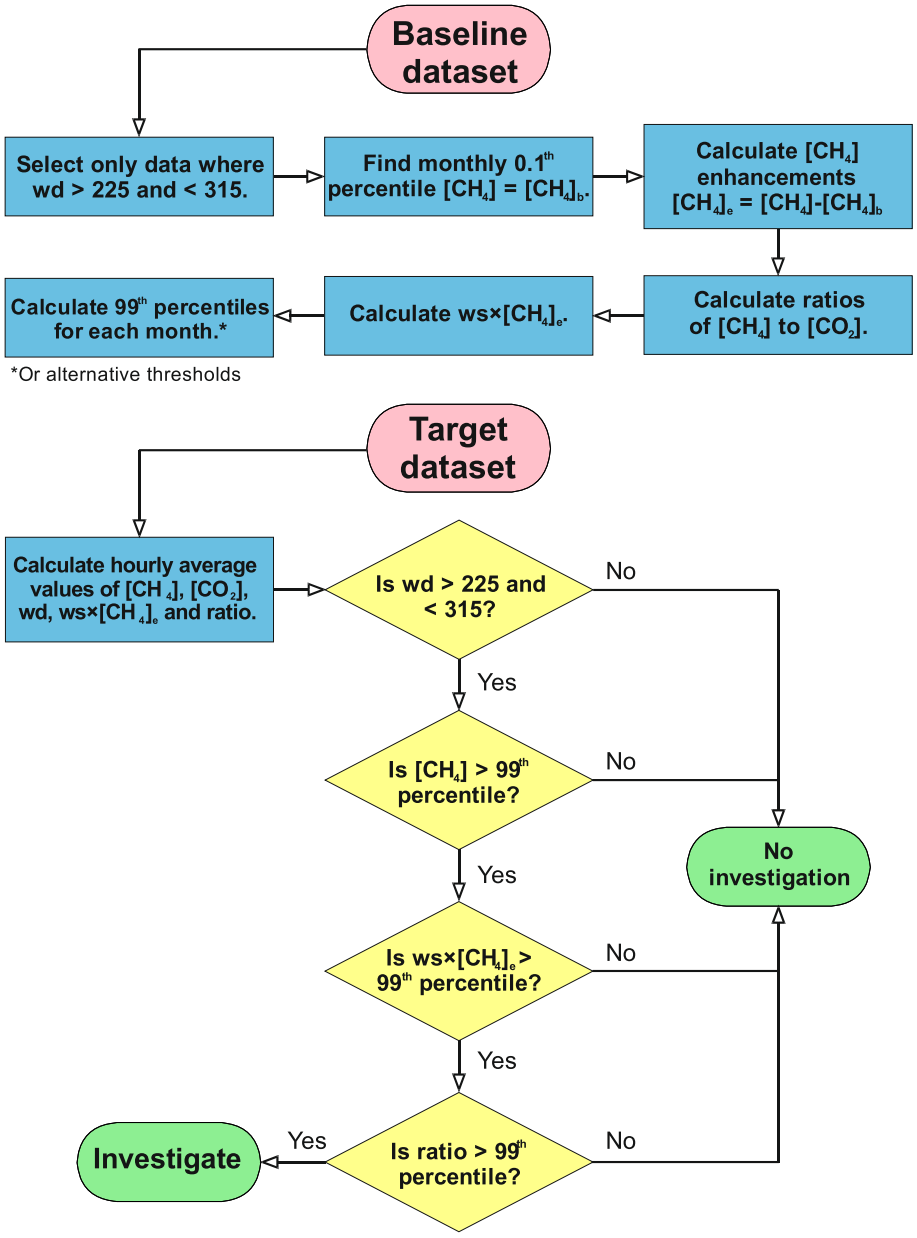

Fig. 8. Flow scheme for detecting baseline excursion events. Key to abbreviations: $[CH_4]_b$ = 0.1th percentile $[CH_4]$, $[CH_4]_e$ = $[CH_4]$ enhancement = $[CH_4]$ – $[CH_4]_b$, wd = wind direction, ws = wind speed. Wind directions between 225° and 315° incorporate all winds that can be considered to be westerly winds (i.e. 270° ± 45°).

perfect but that approximately 10 in every 17,500 h (0.05%) may exceed the threshold criteria regardless of operational activity. These periods were generally associated with extremely low wind speeds (<1 m s^{-1}), or rapidly changing meteorological conditions.

The periods that exceeded the threshold criteria at KM were confirmed (by the operators) to be associated with emissions from the pre-existing well head. Fig. 9 shows 30-minute averaged [CH_4], [CO_2], ratio [CH_4]:[CO_2], wind speed, wind speed×[CH_4]$_e$ and wind direction. The periods highlighted in red (4th and 17th March) exceeded the threshold criteria. Two large excursions in CH_4 mixing ratios were observed, with no concurrent increases in [CO_2], under moderately high wind speeds (>3 m s^{-1}) and with a wind direction predominantly from the west. The position of the existing well-head to the south-west of the monitoring station may mean that emissions from this well-head are occasionally missed by the westerly-wind specific criteria in Fig. 8.

The identification of these events at the site in Kirby Misperton clearly demonstrates the power of the threshold criteria and illustrates that they will be useful in diagnosing future emissions during operational activity.

4.4. Gaussian plume modelling

Gaussian plume modelling was used as an example test of the efficacy of the threshold criteria for identifying emissions from shale gas extraction facilities. A number of emission scenarios were simulated by solving a 3-D advection-diffusion equation (Connolly, 2019).

The Gaussian plume simulation examples described here were performed for a baseline station characteristically similar to that at PNR; that is, one that is roughly 350 m downwind (in the prevailing wind direction) of the shale gas well-head. Various different wind speed parameters, between 3 and 12 m s^{-1}, were tested to determine the impact that certain meteorological conditions had on the observed CH_4 enhancement at the site. Different CH_4 source strengths, between 1 and 100 g s^{-1}, were also used. Analogous simulations for the measurement station location relative to the shale gas site at KM were not possible due to the close proximity of the measurement station to the well-head (<50 m).

Table 3 provides a set of simulated CH_4 enhancements at the baseline station given different sets of meteorological conditions and emission source strengths. The simulations assumed that the ground-based monitoring station was positioned at the centre of the Gaussian-shaped plume, emitted from a ground-level source. Given the rather crude assumption that the monitoring station lies at the centre of the Gaussian-shaped plume means that the results presented in Table 3 represent maximum possible values under the stated conditions. Neutral meteorological stability conditions, which best reflect the observed meteorology, were used in simulations and surface roughness was ignored for simplicity. Simulated enhancements under different meteorological conditions are provided in the Supplementary Information; these should not be used as an indication of the uncertainty of the values provided in Table 3.

5. Conclusions and implications

A comprehensive set of greenhouse gas measurement data were recorded alongside meteorological parameters at two sites intended for the extraction of shale gas using hydraulic fracturing. These measurements were recorded in the two years prior to any operational activity in order to provide a background (or baseline) record of local and regional CH_4 and CO_2 mixing ratios ahead of the commencement of hydraulic fracturing for shale gas exploration.

Identifying excursions from the observed baseline conditions due to CH_4 emissions is of utility to regulators, site operators and the general public. An algorithmic set of guidelines for the potential identification of such emissions was developed and tested against the baseline dataset, confirming the observation of CH_4 emissions from a pre-existing well-head on the KM site. Gaussian plume simulations were used to provide further context to the measurements at PNR; potential CH_4 enhancements measured at the station were linked to approximate upper-limits for emission source strength under defined meteorological conditions. The same simulations were not performed for KM due to the close proximity of the measurement station and the well-head, demonstrating the necessity of appropriate positioning of measurement stations.

This work represents an international first for large scale baseline measurement of CH_4 and CO_2 at a shale gas site. The climatologies provide a reference against which emissions events can be detected and attributed in analogous monitoring conducted during operational shale gas site activity at both the PNR and KM sites. Important suggestions for future baseline projects include:

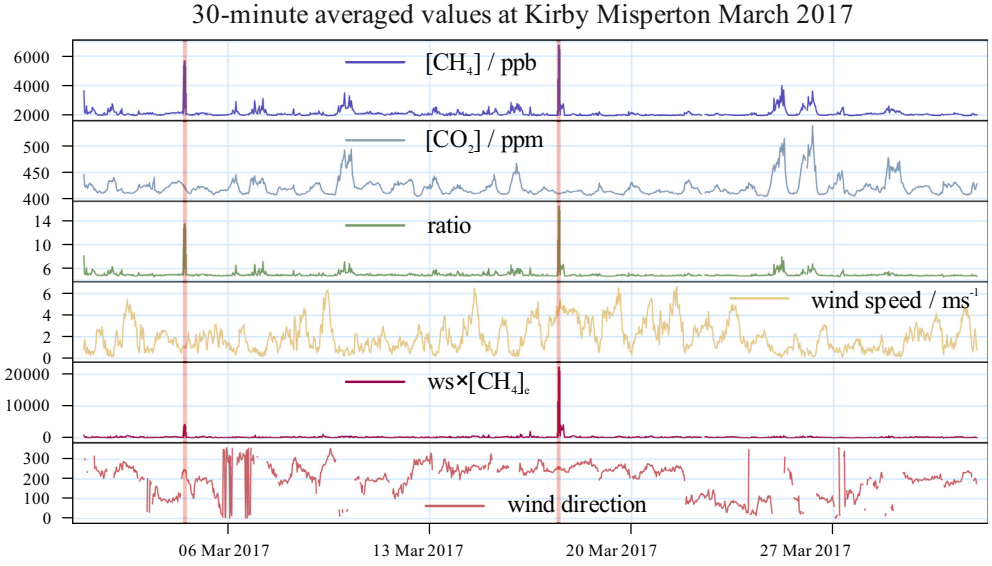

Fig. 9. 30-minute averaged data ([CH_4]/ppb, [CO_2]/ppm, ratio [CH_4]:[CO_2], wind speed/m s^{-1}, wind speed×[CH_4]$_e$/ppb m s^{-1}, wind direction) at Kirby Misperton in March 2017. The red highlighted periods exceeded the threshold criteria provided in Fig. 8.

Table 3
Simulated CH_4 enhancements above the background at PNR provided different meteorological conditions and emission source strength. Enhancements were simulated using Gaussian plume modelling, under the assumption that the enhancement occurred at the centre of a plume 350 m downwind of the emission source.

CH_4 source strength/g s^{-1}	Wind speed/m s^{-1}			
	3	6	9	12
	CH_4 enhancement above background/ppb			
1	438	219	146	109
2	730	365	243	182
3	1218	609	406	304
5	2031	1016	677	508
8	3388	1694	1129	847
13	5651	2826	1884	1413
22	9427	4714	3142	2357
36	15,725	7863	5242	3931
60	26,231	13,116	8744	6558
100	43,757	21,878	14,586	10,939

This reference table could be used as a quick-look guide for future observations in similar conditions but should not be treated as a substitute for a more in-depth case study analysis, where parameters could be explicitly defined for improved flux modelling. Given that the above enhancements were simulated with several major assumptions, they should be treated as maximum possible enhancements under the stated conditions. Regardless, the simulated enhancement was linearly dependent on both wind speed and source strength, with the largest enhancements simulated under low wind speeds and with high emissions, as expected.

1. Calibration and maintenance of equipment: long-term field monitoring of environmental parameters necessitates continued quality control of all measured data. Robust and regular calibration procedures of all on-site equipment should be performed, alongside the calibration and maintenance of any replacement equipment. Calibrations should be performed for each instrument as individual calibration factors may not be representative for all equipment. The necessary timescale for repeat calibrations should be determined according to an assessment of the key factors driving instrument drift on a case-by-case basis. As a guide, calibrations related to this work were performed at intervals between no less than three weeks and no more than three months.
2. Meteorological: the concentrations of atmospheric constituents are highly dependent on meteorological conditions. Hence concurrent measurements of meteorology are required to make assessments of baseline parameters as a function of those conditions. This can help to elucidate the sources of local and regional pollution.
3. Temporal scale: the authors recommend performing baseline measurements for at least one year prior to any operational activity due to the large variability in conditions on a seasonal basis. However, significant variability in yearly conditions cannot be ruled out by measuring for a period of a single year, especially if any additional new nearby emission sources (e.g. other industrial development) may be expected to impact the local area between the period of baseline evaluation and operational monitoring.
4. Threshold criteria: the production of threshold criteria for the identification of extreme events requires careful assessment of the baseline data. Criteria for the determination of baseline excursions at the two sites assessed as part of this work are provided in Fig. 8. These criteria utilised statistical analyses based on a dynamic baseline, thereby providing robust measures against which future emissions can be detected. Correct baseline interpretation and extensive statistical analyses are crucial for the determination of useful threshold criteria.
5. Gaussian plume modelling: simulations of the CH_4 enhancements expected at the PNR measurement station under defined meteorological conditions and given different emission source strengths may add further context to any identified CH_4 excursions in the future. This type of analysis was not possible at KM due to the sub-optimal location of the measurement station relative to the wellhead.

CRediT authorship contribution statement

Jacob T. Shaw: Methodology, Validation, Formal analysis, Investigation, Data curation, Writing - original draft, Writing - review & editing. **Grant Allen:** Conceptualization, Validation, Investigation, Writing - original draft, Writing - review & editing, Supervision, Project administration. **Joseph Pitt:** Methodology, Validation, Formal analysis, Investigation, Data curation, Writing - review & editing. **Mohammed I. Mead:** Conceptualization, Methodology, Investigation, Writing - review & editing. **Ruth M. Purvis:** Conceptualization, Methodology, Investigation, Writing - review & editing, Project administration. **Rachel Dunmore:** Investigation, Writing - review & editing. **Shona Wilde:** Investigation. **Adil Shah:** Investigation. **Patrick Barker:** Investigation. **Prudence Bateson:** Investigation. **Asan Bacak:** Investigation. **Alastair C. Lewis:** Conceptualization, Writing - review & editing. **David Lowry:** Conceptualization, Investigation, Writing - review & editing. **Rebecca Fisher:** Investigation. **Mathias Lanoiselle:** Investigation. **Robert S. Ward:** Conceptualization, Methodology, Validation, Writing - review & editing, Supervision, Project administration, Funding acquisition.

CRediT authorship contribution statement

Jacob T. Shaw: Methodology, Validation, Formal analysis, Investigation, Data curation, Writing - original draft, Writing - review & editing. **Grant Allen:** Conceptualization, Validation, Investigation, Writing - original draft, Writing - review & editing, Supervision, Project administration. **Joseph Pitt:** Methodology, Validation, Formal analysis, Investigation, Data curation, Writing - review & editing. **Mohammed I. Mead:** Conceptualization, Methodology, Investigation, Writing - review & editing. **Ruth M. Purvis:** Conceptualization, Methodology, Investigation, Writing - review & editing, Project administration. **Rachel Dunmore:** Investigation, Writing - review & editing. **Shona Wilde:** Investigation. **Adil Shah:** Investigation. **Patrick Barker:** Investigation. **Prudence Bateson:** Investigation. **Asan Bacak:** Investigation. **Alastair C. Lewis:** Conceptualization, Writing - review & editing. **David Lowry:** Conceptualization, Investigation, Writing - review & editing. **Rebecca Fisher:** Investigation. **Mathias Lanoiselle:** Investigation. **Robert S. Ward:** Conceptualization, Methodology, Validation, Writing - review & editing, Supervision, Project administration, Funding acquisition.

Acknowledgements

The information reported here has been collected as part of the BGS-led environmental monitoring project (http://www.bgs.ac.uk/lancashire). This project is jointly funded by the British Geological Survey's National Capability programme and a grant awarded by the Department for Business, Energy and Industrial Strategy (BEIS; Grant code: GA/18F/017/NEE6617R). BGS authors publish with the permission of the Executive Director, BGS NERC-UKRI.

Appendix A. Supplementary data

Supplementary data to this article can be found online at https://doi.org/10.1016/j.scitotenv.2019.05.266.

References

Allen, D.T., 2016. Emissions from oil and gas operations in the United States and their air quality implications. J. Air Waste Manag. Assoc. 66 (6), 549–575. https://doi.org/10.1080/10962247.2016.1171263.

Alvarez, R.A., Zavala-Araiza, D., Lyon, D.R., Allen, D.T., Barkley, Z.R., Brandt, A.R., Davis, K.J., Herndon, S.C., Jacob, D.J., Karion, A., Kort, E.A., Lamb, B.K., Lauvaux, T., Maasakkers, J.D., Marchese, A.J., Omara, M., Pacala, S.W., Peischl, J., Robinson, A.L., Shepson, P.B., Sweeney, C., Townsend-Small, A., Wofsy, S.C., Hamburg, S.P., 2018. Assessment of methane emissions from the U.S. oil and gas supply chain. Science 361, eaar7204. https://doi.org/10.1126/science.aar7204.

Burnham, A., Han, J., Clark, C.E., Wang, M., Dunn, J.B., Palou-Rivera, I., 2012. Life-cycle greenhouse gas emissions of shale gas, natural gas, coal, and petroleum. Environ. Sci. Technol. 46, 619–627. https://doi.org/10.1021/es201942m.

Connolly, P., 2019. A simple Gaussian plume model for investigating air quality. https://github.com/maul1609/gaussian-plume-model-practical, Accessed date: 2 July 2019.

Darrah, T.H., Vengosh, A., Jackson, R.B., Warner, N.R., Poreda, R.J., 2014. Noble gases identify the mechanisms of fugitive gas contamination in drinking-water wells overlying the Marcellus and Barnett Shales. Proc. Natl. Acad. Sci. U. S. A. 111, 14076–14081. https://doi.org/10.1073/pnas.1322107111.

Dlugokencky, E., 2019. NOAA/ESRL. http://www.esrl.noaa.gov/gmd/ccgg/trend, Accessed date: 1 October 2019.

Edwards, P.M., Brown, S.S., Roberts, J.M., Ahmadov, R., Banta, R.M., de Gouw, J.A., Dubé, W.P., Field, R.A., Flynn, J.H., Gilman, J.B., Graus, M., Helmig, D., Koss, A., Langford, A.O., Lefer, B.L., Lerner, B.M., Li, R., Li, S.-M., McKeen, S.A., Murphy, A.M., Parrish, D.D., Senff, C.J., Soltis, J., Stutz, J., Sweeney, C., Thompson, C.R., Trainer, M.K., Tsai, C., Veres, P.R., Washenfelder, R.A., Warneke, C., Wild, R.J., Young, C.J., Yuan, B., Zamora, R., 2014. High winter ozone pollution from carbonyl photolysis in an oil and gas basin. Nature 514, 351–354. https://doi.org/10.1038/nature13767.

Field, R.A., Soltis, J., Murphy, S., 2014. Air quality concerns of unconventional oil and natural gas production. Environ. Sci.: Processes Impacts 16, 954–969. https://doi.org/10.1039/C4EM00081A.

Frohlich, C., 2012. Two-year survey comparing earthquake activity and injection-well locations in the Barnett Shale, Texas. Proc. Natl. Acad. Sci. U. S. A. 109, 13934–13938. https://doi.org/10.1073/pnas.1207728109.

Hildenbrand, Z.L., Mach, P.M., McBride, E.M., Dorreyatim, M.N., Taylor, J.T., Carlton Jr., D.D., Meik, J.M., Fontenot, B.E., Wright, K.C., Schug, K.A., Verbeck, G.F., 2016. Point source attribution of ambient contamination events near unconventional oil and gas development. Sci. Total Environ. 573, 382–388. https://doi.org/10.1016/j.scitotenv.2016.08.118.

Howarth, R.W., 2015. Methane emissions and climatic warming risk from hydraulic fracturing and shale gas development: implications for policy. Energy Emission Control Technol. 3, 45–54. https://doi.org/10.2147/EECT.S61539.

Jenner, S., Lamadrid, A.J., 2013. Shale gas vs. coal: policy implications from environmental impact comparisons of shale gas, conventional gas, and coal on air, water, and land in the United States. Energ Policy 53, 442–453. https://doi.org/10.1016/j.enpol.2012.11.010.

Konschnik, K., Jordaan, S.M., 2018. Reducing fugitive methane emissions from the North American oil and gas sector: a proposed science-policy framework. Clim. Pol. 18, 1133–1151. https://doi.org/10.1080/14693062.2018.1427538.

Kozłowska, M., Brudzinski, M.R., Friberg, P., Skoumal, R.J., Baxter, N.D., Currie, B.S., 2018. Maturity of nearby faults influences seismic hazard from hydraulic fracturing. Proc. Natl. Acad. Sci. U. S. A. 115, E1720–E1729. https://doi.org/10.1073/pnas.1715284115.

Lan, X., Talbot, R., Laine, P., Torres, A., 2015. Characterizing fugitive methane emissions in the Barnett shale area using a mobile laboratory. Environ. Sci. 49, 8139–8146. https://doi.org/10.1021/es5063055.

Littlefield, J.A., Marriott, J., Schivley, G.A., Skone, T.J., 2017. Synthesis of recent ground-level methane emission measurements from the US natural gas supply chain. J. Clean. Prod. 148, 118–126. https://doi.org/10.1016/j.jclepro.2017.01.101.

Myhre, G., Shindell, D., Bréon, F.-M., Collins, W., Fuglestvedt, J., Huang, J., Koch, D., Lamarque, J.-D., Lee, D.S., Mendoza, B., Nakajima, T., Robock, A., Stephens, G., Takemura, T., Zhang, H., Jacob, D., Ravishankara, A.R., Shine, K., 2013. Anthropogenic and natural radiate forcing. In: Stocker, T.F., et al. (Eds.), Climate Change 2013: The Physical Science Basis, Contribution of Working Group I to the Fifth Assessment Report of the Intergovernmental Panel on Climate Change. Cambridge University Press, Cambridge, United Kingdom and New York, NY.

O'Shea, S.J., Bauguitte, S.J.-B., Gallagher, M.W., Lowry, D., Percival, C.J., 2013. Development of a cavity-enhanced absorption spectrometer for airborne measurements of CH_4 and CO_2. Atmos. Meas. Tech. 6, 1095–1109. https://doi.org/10.5194/amt-6-1095-2013.

Peischl, J., Eilerman, S.J., Neuman, J.A., Aikin, K.C., de Gouw, J., Gilman, J.B., Herndon, S.C., Nadkarni, R., Trainer, M., Warneke, C., Ryerson, T.B., 2018. Quantifying methane and ethane emissions to the atmosphere from Central and Western U.S. oil and natural gas production regions. J. Geophys. Res.-Atmos. 123, 7725–7740. https://doi.org/10.1029/2018JD028622.

Prinn, R.G., Weiss, R.F., Arduini, J., Arnold, T., DeWitt, H.L., Fraser, P.J., Ganesan, A.L., Gasore, J., Harth, C.M., Hermansen, O., Kim, J., Krummel, P.B., Li, S., Loh, Z.M., Lunder, C.R., Maione, M., Manning, A.J., Miller, B.R., Mitrevski, B., Mühle, J., O'Doherty, S., Park, S., Reimann, S., Rigby, M., Saito, T., Salameh, P.K., Schmidt, R., Simmonds, P.G., Steele, L.P., Vollmer, M.K., Wang, R.H., Yao, B., Yokouchi, Y., Young, D., Zhou, L., 2018. History of chemically and radiatively important atmospheric gases from the Advanced Global Atmospheric Gases Experiment (AGAGE). Earth Syst. Sci. Data 10, 985–1018. https://doi.org/10.5194/essd-10-985-2018.

Purvis, R.M., Lewis, A.C., Hopkins, J.R., Wilde, S.E., Dunmore, R.E., Allen, G., Pitt, J., Ward, R.S., 2019. Effects of pre-fracking operations on ambient NO_x at a UK rural well-site. Sci. Total Environ. 673, 445–454. https://doi.org/10.1016/j.scitotenv.2019.04.077.

Rogelj, J., Shindell, D., Jiang, K., Fifita, S., Forster, P., Ginzburg, V., Handa, C., Kheshgi, H., Kobayashi, S., Kriegler, E., Mundaca, L., Séférian, R., Vilariño, M.V., 2018. Mitigation pathways compatible with 1.5°C in the context of sustainable development. In: Global Warming of 1.5°C. an IPCC Special Report on the Impacts of Global Warming of 1.5°C Above Pre-Industrial Levels and Related Global Greenhouse Gas Emission Pathways, in the Context of Strengthening the Global Response to the Threat of Climate Change, Sustainable Development, and Efforts to Eradicate Poverty [Masson-Delmotte, V., Zhai, P., Pörtner, O., Roberts, D., Skea, J., Shukla, P.R., Pirani, A., Moufama-Okia, W., Péan, C., Pidcock, R., Connors, S., Matthews, J.B.R., Chen, Y., Zhou, X., Gomis, M.I., Lonnoy, E., Maycock, T., Tignor, M., Waterfield, T. (eds.)]. (In Press).

Schneising, O., Burrows, J.P., Dickerson, R.R., Buchwitz, M., Reuter, M., Bovensmann, H., 2014. Remote sensing of fugitive methane emissions from oil and gas production in North American tight geologic formations. Earth's Future 2, 548–558. https://doi.org/10.1002/2014EF000265.

Vidic, R.D., Brantley, S.L., Vandenbossche, J.M., Yoxtheimer, D., Abad, J.D., 2013. Impact of shale gas development on regional water quality. Science 340, 1235009. https://doi.org/10.1126/science.1235009.

Ward, R.S., Smedley, P.L., Allen, G., Baptie, B.J., Daraktchieva, Z., Horleston, A., Jones, D.G., Jordan, C.J., Lewis, A., Lowry, D., Purvis, R.M., Rivett, M.O., 2017. Environmental Baseline Monitoring Project: Phase II Final Report. British Geological Survey, Nottingham, UK (163 pp. (OR/17/049) (Unpublished)).

Ward, R.S., Smedley, P.L., Allen, G., Baptie, B.J., Cave, M.R., Daraktchieva, Z., Fisher, R., Hawthorn, D., Jones, D.G., Lewis, A., Lowry, D., Luckett, R., Marchant, B.P., Purvis, R.M., Wilde, S., 2018. Environmental Baseline Monitoring: Phase III Final Report (2017–2018). British Geological Survey, Nottingham, UK (143pp. (OR/18/026) (Unpublished)).

Zavala-Araiza, D., Lyon, D., Alvarez, R.A., Palacios, V., Harriss, R., Lan, X., Talbot, R., Hamburg, S.P., 2015. Toward a functional definition of methane super-emitters: application to natural gas production sites. Environ. Sci. Technol. 49, 8167–8174. https://doi.org/10.1021/acs.est.5b00133.

Zavala-Araiza, D., Alvarez, R.A., Lyon, D.R., Allen, D.T., Marchese, A.J., Zimmerle, D.J., Hamburg, S.P., 2017. Super-emitters in natural gas infrastructure are caused by abnormal process conditions. Nat. Commun. 8, 14012. https://doi.org/10.1038/ncomms14012.